

# CALCULATING THE DISPERSION DIAGRAM USING THE NONORTHOGONAL FDTD METHOD

W. Song, Y. Hao and C. G. Parini

Department of Electronic Engineering, Queen Mary University of London  
Mile End Road, London E1 4NS, UK  
E-mail: y.hao@elec.qmul.ac.uk

**Keywords:** Finite-difference time domain (FDTD), Electromagnetic bandgap structure (EBG), Nonorthogonal FDTD (NFDTD) Method.

## Abstract

This paper presents a Nonorthogonal Finite-Difference Time-Domain (NFDTD) modelling of Photonic Bandgap (PBG) structures. The NFDTD method discretise the curved structures in a conformal way. As a result, when the curved elements or oblique surfaces are involved in the EBG structure, the NFDTD scheme requires much fewer cells compared with the conventional Yee's scheme. Consequently the requirement of the computer memory and the computation time can be reduced.

## 1 Introduction

Electromagnetic bandgap (EBGs) structures are studied using a variety of methods including the plane wave expansion method [1], generalized Rayleigh identity method [2], transfer matrix method [3], *etc.* Among them, the Finite-Difference Time-Domain (FDTD) method is a widely used method for EBG structure modelling because of its simplicity in algorithm and capability to model complex structures with wide frequency band solutions. In previous FDTD approaches, an overwhelming majority is based on the Yee's scheme [4-6], using uniform orthogonal meshes. There is also an alternative FDTD approach developed in the nonorthogonal coordinate system [8], in which the dispersion diagram is obtained using a uniform rhombic grid in order to model a rhombic unit cell. In that approach, the formulas are derived from the conventional Yee's scheme with adjustments for the fixed skewed angle in the grid. However, when the curved unit cell element is considered, staircasing approximation is employed, either with an orthogonal grid [4-7] or with a rhombic grid [8]. It is anticipated that the staircasing approximation will cause numerical errors when the wavelength of interest is small with

regard to the cell size. Consequently, a dense grid with high spatial resolution is required and hence leads to extensive computation with large computer memory requirement.

On the other hand, the nonorthogonal FDTD (NFDTD) scheme originated by Holland in 1983 [9] uses structured meshes when modelling curved structures. Compared to the staircase FDTD scheme, fewer meshes are needed to represent the curved or oblique boundary of electromagnetic structures. However, it has been reported that the NFDTD scheme suffers the late time instability which is inherent in the algorithm [10].

In this paper, two infinite two-dimensional structures namely metallic cylinder rods loaded periodically in free space and air holes periodically embedded in dielectric background are modelled as examples to demonstrate the modelling of the EBG structure using the NFDTD scheme. Dispersion diagrams of these EBG structures are plotted. The numerical accuracy and the requirements on the spatial resolution are compared with the conventional Yee's scheme.

## 2 NFDTD Modelling of the EBG Structure

### 2.1 NFDTD Algorithm

Maxwell's curl equations in linear, isotropic, nondispersive, lossy materials:

$$\begin{aligned}\frac{\partial \vec{H}}{\partial t} &= -\frac{1}{\mu} \nabla \times \vec{E} - \frac{1}{\mu} (\vec{M}_{source} + \sigma^* \vec{H}) ; \\ \frac{\partial \vec{E}}{\partial t} &= -\frac{1}{\varepsilon} \nabla \times \vec{H} - \frac{1}{\varepsilon} (\vec{J}_{source} + \sigma \vec{E}) ;\end{aligned}\quad (1)$$

To deal with the electric and magnetic field quantities on a nonorthogonal grid, two different local coordinate

systems are used: the normal basis vectors  $\{\vec{a}_i\}(i=1, 2, 3)$ , and the reciprocal basis vectors  $\{\vec{a}^i\}(i=1, 2, 3)$ .

The reciprocal basis related to the unitary basis as:

$$\vec{a}^1 = \frac{\vec{a}_2 \times \vec{a}_3}{\sqrt{g}}; \quad \vec{a}^2 = \frac{\vec{a}_3 \times \vec{a}_1}{\sqrt{g}}; \quad \vec{a}^3 = \frac{\vec{a}_1 \times \vec{a}_2}{\sqrt{g}}; \quad (2)$$

where

$$\sqrt{g} = \vec{a}_1 \cdot \vec{a}_2 \times \vec{a}_3 \quad (3)$$

is the volume enclosed by the unit cell.

Then, an arbitrary vector can be expressed by:

$$\vec{E} = \sum_{i=1}^3 e^i \vec{a}_i = \sum_{i=1}^3 e_i \vec{a}^i \quad (4)$$

And the relationship holds:

$$\vec{a}_i \cdot \vec{a}^j = \delta_{i,j}$$

where  $\delta$  is Kronecker delta:

$$\delta_{i,j} = \begin{cases} 1(i=j) \\ 0(i \neq j) \end{cases} \quad (5)$$

The operation of curl in the nonorthogonal coordinates can be written as [19]:

$$\nabla \times A = \frac{1}{\sqrt{g}} \sum_{i=1}^3 [(\vec{a}_j \cdot A_i) \vec{a}_k - (\vec{a}_k \cdot A_i) \vec{a}_j] \quad (6)$$

If a contravariant base vector  $\vec{a}^m$  ( $m=1, 2, 3$ ) is used to perform a scalar dot product of equation (6), equation (6) becomes:

$$\nabla \times A \cdot \vec{a}^m = \frac{1}{\sqrt{g}} \sum_{i=1}^3 [(\vec{a}_j \cdot A_i) (\vec{a}_k \cdot \vec{a}^m) - (\vec{a}_k \cdot A_i) (\vec{a}_j \cdot \vec{a}^m)] \quad (7)$$

(i, j, k in ascending order)

Taking  $m=1$  for example:

$$\begin{aligned} \nabla \times A \cdot \vec{a}^1 &= \frac{1}{\sqrt{g}} \sum_{i=1}^3 [(\vec{a}_j \cdot A_i) (\vec{a}_k \cdot \vec{a}^1) - (\vec{a}_k \cdot A_i) (\vec{a}_j \cdot \vec{a}^1)] \\ &= \frac{1}{\sqrt{g}} \sum_{i=1}^3 [(\vec{a}_3 \cdot A_2) - (\vec{a}_2 \cdot A_3)] \\ &= \frac{1}{\sqrt{g}} \left[ \frac{\partial A_3}{\partial u^2} - \frac{\partial A_2}{\partial u^3} \right] \end{aligned} \quad (7a)$$

Equation (7) is the basis of Holland's (conventional) differential equations.

## 2.2 Model Parameter

Two types lattices, namely a square lattice and triangular one are simulated in terms of TE and TM

polarization respectively using different spatial resolution.

In the metallic rods modelling, the material of rods is chosen as copper with relative permittivity  $\epsilon_r = 1$  and conductivity  $\sigma = 5.8 \times 10^7$  S/m. The ratio of the radius ( $r$ ) to the lattice constant ( $a$ ) is  $r/a = 0.2$ .

In the modelling of the air hole embedded in dielectric background, the dielectric material is with relative permittivity  $\epsilon_r = 8.9$ . The ratio of the radius ( $r$ ) to the lattice constant ( $a$ ) is  $r/a = 0.2$ .

## 2.3 Conformal Mesh

The unit cell can be meshed with different spatial resolution using a NFDTD algorithm. Figure 1 shows examples of  $18 \times 18$  (for square lattice) and  $18 \times 15$  (for rhombic/ triangular lattice) NFDTD grid. As is the case of the conventional Yee's FDTD scheme, a denser mesh can often provide a more accurate result.

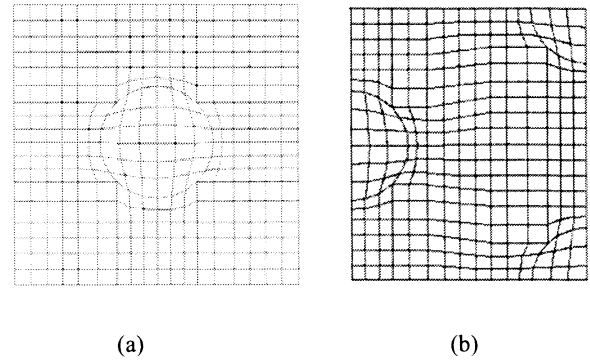


Fig. 1 Mesh schemes for the unit cells of the PBG structures in NFDTD grid. (a)  $18 \times 18$  for square lattice; (b)  $18 \times 15$  for triangular lattice;

## 2.4 Boundary Condition

Since the the EBG structure is periodic, the fields should satisfy the Bloch theory, i.e., the fields can be written in the following Bloch form:

$$\vec{E}(\vec{r}) = e^{i\vec{k} \cdot \vec{r}} \cdot \vec{e}(\vec{r}); \quad \vec{H}(\vec{r}) = e^{i\vec{k} \cdot \vec{r}} \cdot \vec{h}(\vec{r}); \quad (8)$$

where  $\vec{e}(\vec{r})$  and  $\vec{h}(\vec{r})$  are periodic functions in space which means for the lattice vector of  $\vec{L}$ ,

$$\vec{e}(\vec{r} + \vec{L}) = \vec{e}(\vec{r}); \quad \vec{h}(\vec{r} + \vec{L}) = \vec{h}(\vec{r}); \quad (9)$$

Therefore, the Bloch's periodic boundary condition (PBC) at each end of the computation domain are written as:

$$\begin{aligned}
\vec{E}(\vec{r} + \vec{L}) &= e^{i\vec{k} \cdot (\vec{r} + \vec{L})} \cdot \vec{e}(\vec{r} + \vec{L}) \\
&= e^{i\vec{k} \cdot \vec{L}} \cdot e^{i\vec{k} \cdot \vec{r}} \cdot \vec{e}(\vec{r}) \\
&= e^{i\vec{k} \cdot \vec{L}} \cdot \vec{E}(\vec{r}) \quad ; \\
\vec{H}(\vec{r} + \vec{L}) &= e^{i\vec{k} \cdot (\vec{r} + \vec{L})} \cdot \vec{h}(\vec{r} + \vec{L}) \\
&= e^{i\vec{k} \cdot \vec{L}} \cdot e^{i\vec{k} \cdot \vec{r}} \cdot \vec{h}(\vec{r}) \\
&= e^{i\vec{k} \cdot \vec{L}} \cdot \vec{H}(\vec{r}) \quad ; \quad (10)
\end{aligned}$$

## 2.5 Result Processing

The structures are fed with a modulated Gaussian pulse at a random point with different normalized central frequencies in different numerical experiments. The EM fields at random points are monitored and the temporal results are processed by using the Fourier Transformation. On the frequency spectra of each k vector, the resonant frequencies are recorded and plotted against the k vector. In this way, the dispersion diagrams of the modelled PBG structures are plotted and shown in Fig. 2 and Fig. 3.

## 3 Simulation Results

The dispersion diagrams of the proposed EBG structures are obtained from the NFDTD scheme using low spatial resolution (18×18 for square lattice and 18×15 for triangular lattice). The NFDTD results agree well with the conventional Yee's results (shown in Fig.3(b)) and the analytical results by coordinate-space finite-difference method [11].

### 3.1 A Periodic Air Hole in Dielectric Background

Figure 2 plots the dispersion diagrams of the cylindrical air holes periodically embedded in dielectric background in square lattice as an example. Here,  $r/a = 0.2$ .

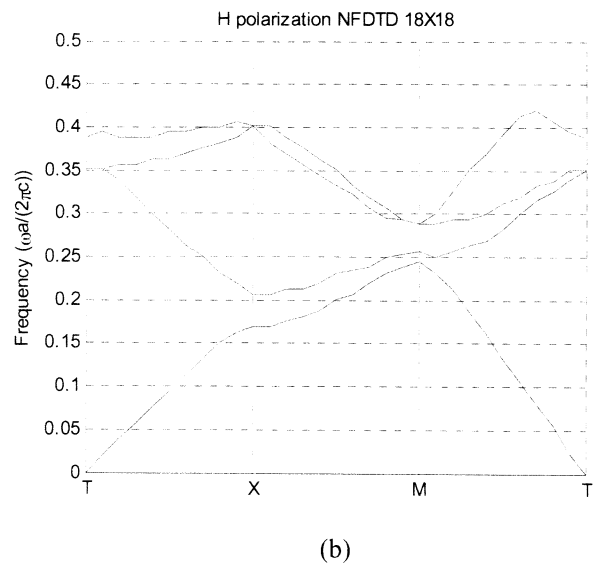
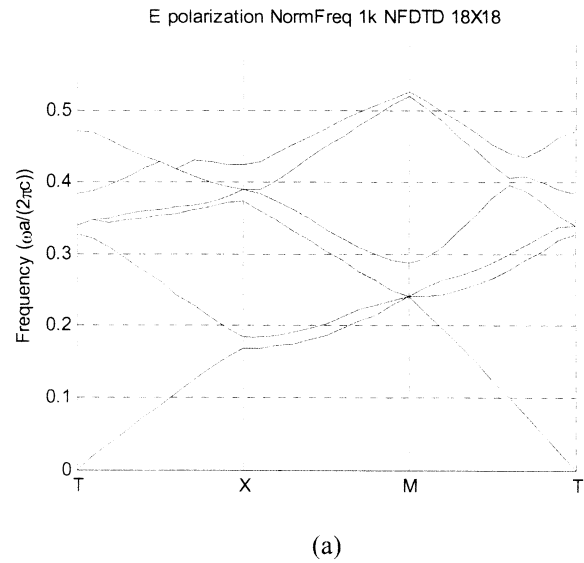


Fig.2 Plots of the several lowest normalized eigenmodes versus the wave vector k for the Air Hole structure in square lattice.  $r/a = 0.2$ . (a) TM mode; (b) TE mode.

### 3.2 Metallic Rods in Free Space – Triangular Lattice

Figure 3 shows the dispersion diagrams of the copper rods in triangular lattice in free space as an example. Here,  $r/a = 0.2$ .

In figure 3 (b), the dispersion diagram from NFDTD with grid size 18×15 is compared with the conventional Yee's FDTD results with a much higher spatial resolution (grid size 80×69). As can be seen, the two results agree well. More numerical experiments show that a minimum of 30×26 grids is required in the simulation using the Yee's FDTD scheme.

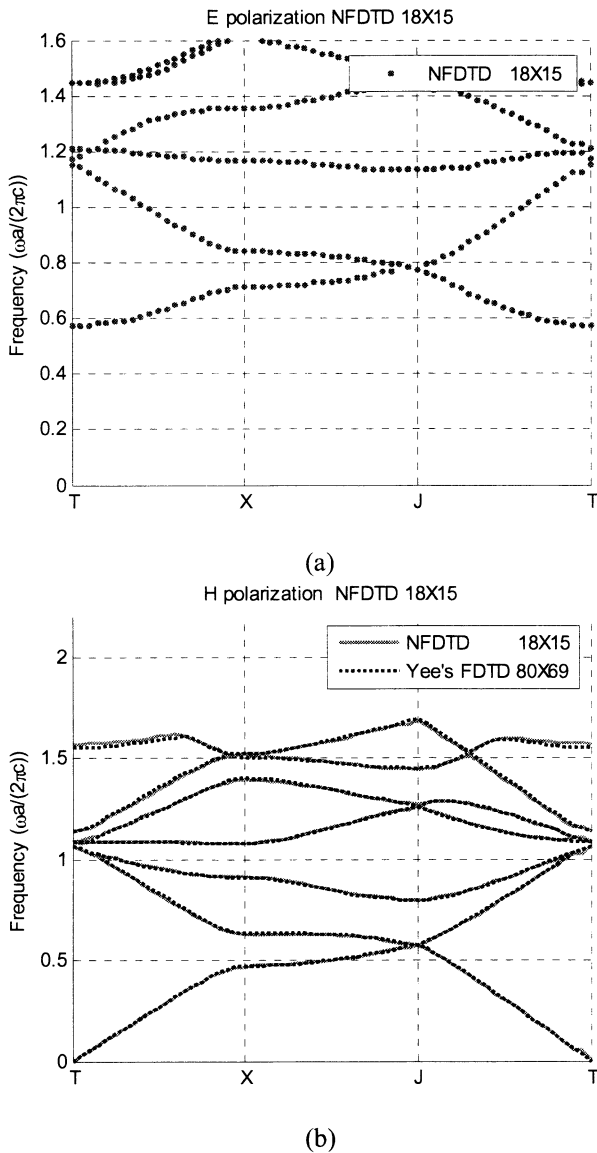


Fig.3 Plots of the several lowest normalized eigenmodes versus the wave vector  $k$  for the copper rods EBG structure in triangular lattice.  $r/a = 0.2$ . (a) TM mode; (b) TE mode – NFDTD result with grid  $18 \times 15$  in comparison with the Yee's FDTD results with grid  $80 \times 69$ .

#### 4 Conclusions

The modelling of EBG structures using the Nonorthogonal FDTD method has been presented in this paper. Two examples namely the metallic rods periodically loaded in free space and the air holes embedded in dielectric background have been simulated in terms of rhombic/triangular lattice and square lattice separately. The dispersion diagrams of the aforementioned structures are presented in terms of TE and TM polarization respectively.

The comparison with the conventional Yee's FDTD approach shows that NFDTD method is able to model curved EBG structure using much coarser meshes without much reduction on the accuracy of the results. In this sense, the requirement on the computer memory and the computation time can be reduced by using the NFDTD method when curved elements are involved in the modelling.

#### References

- [1] K. M. Leung and Y. F. Liu, "Full vector wave calculation of photonic band structures in face-centered-cubic dielectric media", *Phys. Rev. Lett.* Vol. 65, pp. 2646–2649, Nov. 1990.
- [2] N. A. Nicorovici, R. C. McPhedran, and L. C. Botten, "Photonic band gaps for arrays of perfectly conducting cylinders", *Phys. Rev. E*, vol. 52, pp. 1135–1145 Jul. 1995.
- [3] J. B. Pendry and A. MacKinnon "Calculation of photon dispersion relations", *Phys. Rev. Lett.* Vol. 69, pp. 2772–2775 Nov. 1992.
- [4] R. Stoffer, H. J. W. M. Hoekstra, R. M. Deridder, E. Vangroesen and F. P. H. Vanbeckum, "Numerical studies of 2D photonic crystals: Waveguides, coupling between waveguides and filters", *Optical and Quantum Electronics*, Vol. 32, pp. 947-961, 2000.
- [5] A. J. Ward and J. B. Pendry, "Calculating photonic Green's functions using a nonorthogonal finite-difference time-domain method", *Phys. Rev. B*, Vol. 58, pp. 7252–7259, Sep. 1998.
- [6] M. Qiu and S. He, "A nonorthogonal finite-difference time-domain method for computing the band structure of a two-dimensional photonic crystal with dielectric and metallic inclusions", *J. Appl. Phys.* Vol. 87, Issue No: 12, pp. 8268-8275, Jun. 2002.
- [7] X. L. Bao; W. X. Zhang; "The dispersion characteristics of PBG with complex medium by using non-Yee grid higher order FDTD method", *Antennas and Propagation Society International Symposium*, 2003. IEEE, Vol. 2, pp.1128 – 1131, Jun. 2003.
- [8] X. Wang, X. G. Zhang, Q. Yu and B. N. Harmon, "Multiple-scattering theory for electromagnetic waves", *Phys. Rev. B*, Vol. 47, pp. 4161–4167, Feb. 1993.
- [9] R. Holland, "Finite-Difference solution of Maxwell's equations in generalized nonorthogonal coordinates", *IEEE Trans. On Nuclear Science*, NS-30, pp. 4589-4591, 1983

- [10] Y. Hao, V. Douvalis and C. G. Parini, "Reduction of late time instabilities of the finite difference time domain method in curvilinear coordinates", IEE Proceedings-Science, Measurement and Technology, Vol. 149, No. 5, pp. 267-271, Sep. 2002.
- [11] E. I. Smirnova, C. Chen, M. A. Shapiro, J. R. Sirigiri, and R. J. Temkin, "Simulation of photonic band gaps in metal rod lattices for microwave applications ", J. Appl. Phys., Vol 91 No.3, Feb. 2002.